

Jingbo Wang

jingbo.wang@ntnu.no

Odd M. Faltinsen

odd.faltinsen@ntnu.no

Centre for Autonomous Marine Operations and Systems (AMOS), NTNU, Trondheim, Norway

A novel numerical method is proposed for complex potential free-surface flows of incompressible liquids with and without bodies. The present method combines high-order harmonic polynomials with Cartesian grids with local refinement, which can accurately represent highly-deformed free-surface boundaries and complicate body geometries and significantly reduce the errors induced by the space discretization of the governing equations of potential flows, i.e. the Laplace equation. The discretized matrix system is sparse and can be solved efficiently. Combining with proper time-stepping schemes, the present method can stably represent the potential flows in the time domain. These properties make it possible to solve fully nonlinear wave-body interactions in an accurate, stable and efficient manner, for instance, the plunging breakers, water entry of solid objects, and fully nonlinear numerical wave tank (NWT).

Numerical method. The potential flows are governed by the Laplace equations, $\nabla^2\phi = 0$, which are discretized by Cartesian grids with local refinement in the present study. Coarse structured grids are used as the background grids. In the region, where the boundaries are highly curved or the flow changes strongly in space, the grid should be refined. This is achieved by dividing cells into smaller cells until the size of the cells can well capture the curvature of the boundaries and the change of the flows in space. The local solution of the Laplace equations can be represented as $\phi = \sum b_j f_j$. Here, b_j are coefficients and f_j harmonic polynomials, which can be written as $r^n(\cos n\theta, \sin n\theta)$ by the polar coordinates (r, θ) in the 2D space and $R^n P_n^m(\cos \theta)(\cos m\varphi, \sin m\varphi)$ by the spherical coordinates (R, φ, θ) in 3D [1]. The linear equation for a nodal unknown is established by forcing that the local solution is satisfied at the node and the surrounding nodes. Repeating this procedure for all nodal unknowns will result in a sparse linear equation system, which are solved for the velocity potential. In the following sections, the proposed method is employed to solve several important hydrodynamic problems.

Plunging breaker. A plunging breaker was produced by a piston-type wavemaker in a wave tank with the water depth h of 0.6 m [2]. The wavemaker velocity is specified by a non-dimensional Fourier-cosine as $U(t) = \sum_{n=1}^{72} U_n \cos(\omega_n t - \theta_n)$, which is shown in Figure 1. The present simulation reproduces Dommermuth *et al*'s [2] experiments. The numerical free surface is tracked in the Lagrangian manner [3,4] and the grid system is updated at every time step. A numerical plunging breaker is observed in the zone II

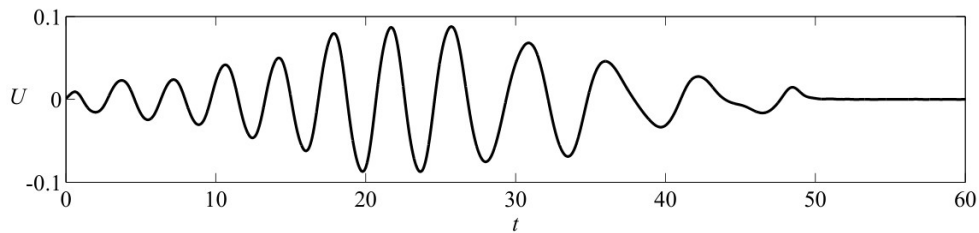


Figure 1. The dimensionless velocity of the piston. The reference length, time and velocity are h , $\sqrt{h/g}$ and \sqrt{gh} respectively.

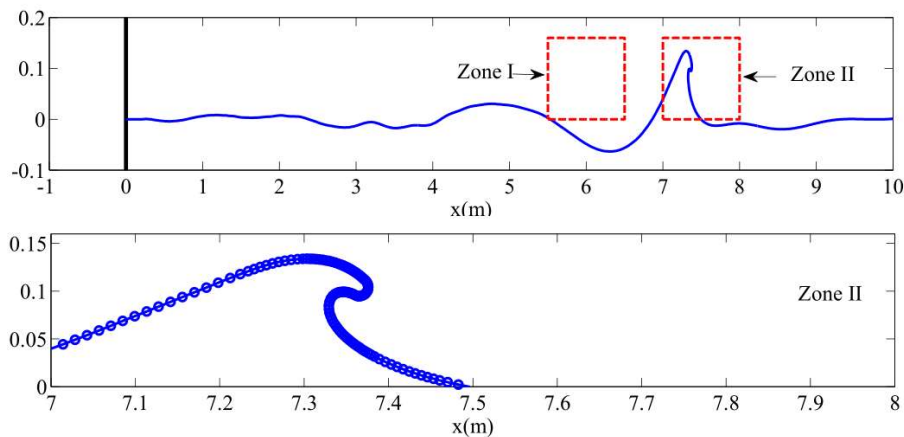


Figure 2. The numerical plunging breaker.

about $t = 12.7s$ as shown in Figure 2. The evolution of the plunging breaker and the dynamic grid system are illustrated in Figure 3.

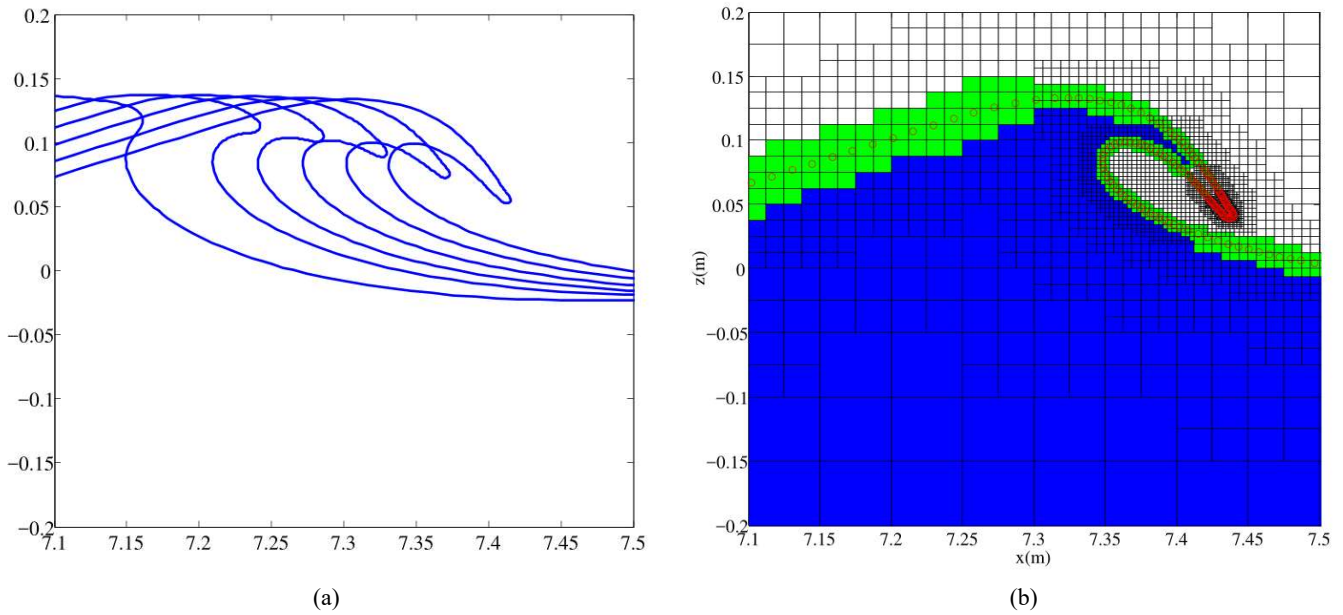


Figure 3. (a) The evolution of the plunging breaker and (b) the numerical grid shortly before the plunging breaker re-enters the water surface.

The conservation of the fluid momentum and energy is checked, which is perfectly satisfied. The wave elevations and fluid velocities are compared to the experiment and good agreements are obtained. Figure 4 illustrates the comparison of wave elevations between the numerical results and the experimental data. It is noted that another plunging breaker is found in the present calculations that was not noted by Dommermuth et al. [2]. It occurs at zone I and is much smaller than the plunging breaker occurring at zone II.

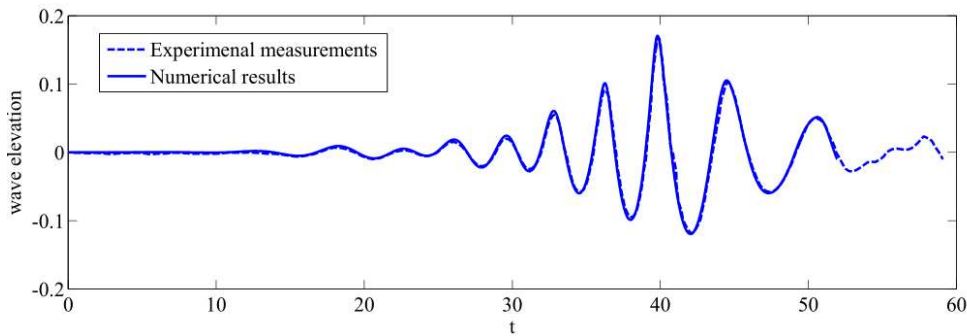


Figure 4. Non-dimensional numerical wave elevations compared to experimental measurements at the non-dimensional $x = 6.67$.

Water entry. A falling wedge with the deadrise angle of β enters the calm water in a constant speed of V , which is shown in Figure

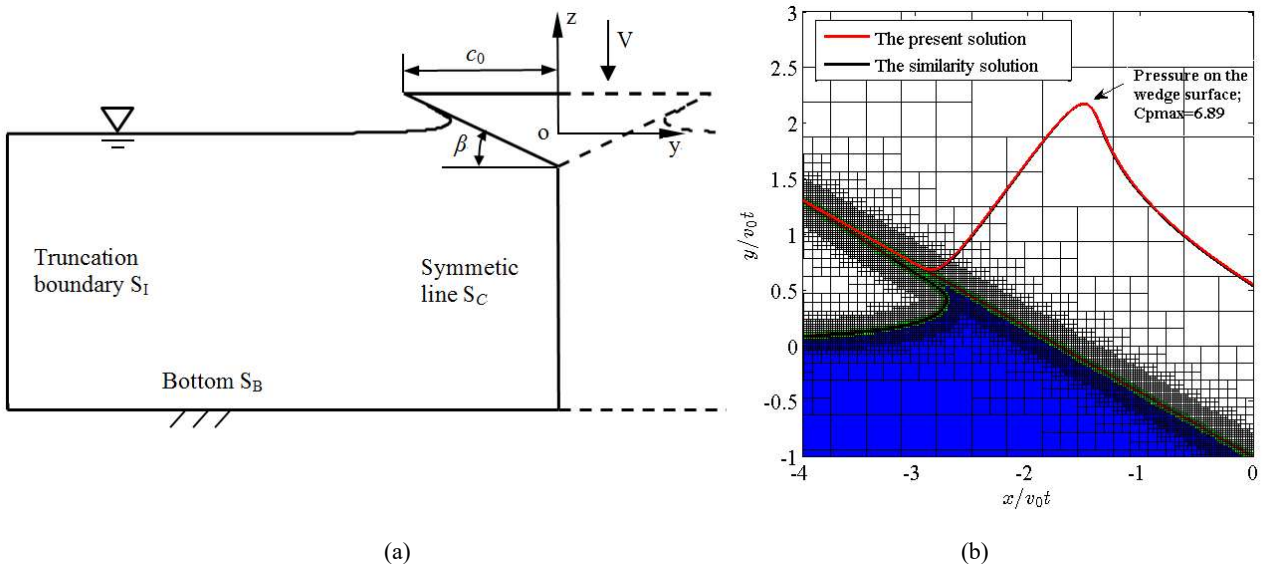


Figure 5. (a) The sketch of the water entry of the wedge and (b) The grid system and the numerical pressure compared to the similarity solution.

5(a). The truncation boundary and the bottom boundary are placed far away from the wedge such that they give negligible influence the flow near the wedge. The viscous effects and the gravity are neglected and then the flow can be analytically represented by the similarity solutions [5]. In the present simulation, the free surface is tracked in the Lagrangian manner [3,4] and the dynamic grid system is used. Figure 5(b) compares the numerical pressure distribution on the wetted wedge surface with the similarity solution for $\beta = 30^\circ$ and the perfect agreement is obtained, which is also achieved when comparing the free surface configuration. Furthermore, good agreements are obtained for the deadrise angles down to 10° .

Travelling ship. The hydrodynamics of travelling ships with and without incoming waves are important and interesting. The present work investigates the ships travelling in the calm water with constant speeds within the framework of the potential flow. In the ship-fixed coordinates system, which has the z -axis upwards and the x -axis coinciding with the course of the ship, the total velocity potential can be represented by the combination of a current and a perturbation velocity potential, i.e. $\Phi = Ux + \phi$. The fully-nonlinear free-surface conditions are considered

$$\frac{\partial \zeta}{\partial t} + \left(U + \frac{\partial \phi}{\partial x} \right) \frac{\partial \zeta}{\partial x} + \frac{\partial \phi}{\partial y} \frac{\partial \zeta}{\partial y} - \frac{\partial \phi}{\partial z} = 0 \quad \text{and} \quad \frac{\partial \phi}{\partial t} + g\zeta + U \frac{\partial \phi}{\partial x} + \frac{1}{2} \left(\left(\frac{\partial \phi}{\partial x} \right)^2 + \left(\frac{\partial \phi}{\partial y} \right)^2 + \left(\frac{\partial \phi}{\partial z} \right)^2 \right) = 0 \quad \text{on } z = \zeta(x, y, t).$$

The Wigley-hull ship model presented in the experiments by Shearer & Cross [6] is studied. The breadth-to-length ratio of the model is 0.1 and the draft-to-length ratio 0.0625. In the numerical simulation, the domain only for $y \geq 0$ is considered because the flow is symmetrical with respect to the plane $y = 0$. The length of the computational domain is six times the ship length L , including $2L$ in the upstream and $3L$ in the downstream. Both the width and height of the computational domain are $3L$. The free surface, out of $-L < x < 2L$ and $y < L$, is set as the damping zone to absorb the outgoing waves. The structured quadrilateral elements with the size of $L/80 \times L/80$ are distributed uniformly on the free surface, which results in 115,200 elements on the surface and about 1,000,000 unknown field points. In the free surface conditions, the terms, $\partial \phi / \partial x$ and $\partial \zeta / \partial x$, are discretized by the upwind scheme and $\partial \phi / \partial y$ and $\partial \zeta / \partial y$ by the central difference scheme. The free surface is tracked in the semi-Lagrangian manner, i.e. only the wave elevations are tracked. Initially, the water is set to be calm. The flow will converge to the steady state with the growth of the time. For $Fn=0.348$, the solutions near the ship hull become almost convergent after about $1.5L/U$. Figure 6 shows the wave profile along the side of the hull. The fully nonlinear method improves the linear solutions near the bow. To improve the numerical solutions furthermore, high-order upwind schemes or finer grids may be considered. We tried the high-order upwind schemes, which improves the solutions compared to the experiments but results in noisy waves in the wakes (the wave pattern is shown in Figure 7). The reasons for the noisy waves are still under investigation. The present calculations are performed on a Laptop computer. The linear solver is very fast: about 400 time steps per minute for the present grid system (the residue is reduced below to 10^{-7}). The nonlinear solver requires updating the matrix system every time step. It reduces the efficiency to 3-4 time steps per minute, which seems still competitive compared to other numerical methods, for instance the Rankine-source method for the fully-nonlinear free surface flows. For the problem, the free-surface conditions are essentially convective equations. Upwind schemes must be used to obtain the correct results. It is natural to use structured quadrilateral elements on the free surface, since the upwind points are well placed and easily found without interpolations. However, the structured grid has two severe drawbacks: the local refinement at highly curved boundaries or the region where the flow changes strongly will results in highly distorted elements, which will reduce the accuracy of the numerical solutions, slow down the convergence and even destroy the numerical solutions; it is very difficult to mesh complex domains by structured grids. To decrease the grid size of the structured elements on the free surface by a factor of 2 will increase

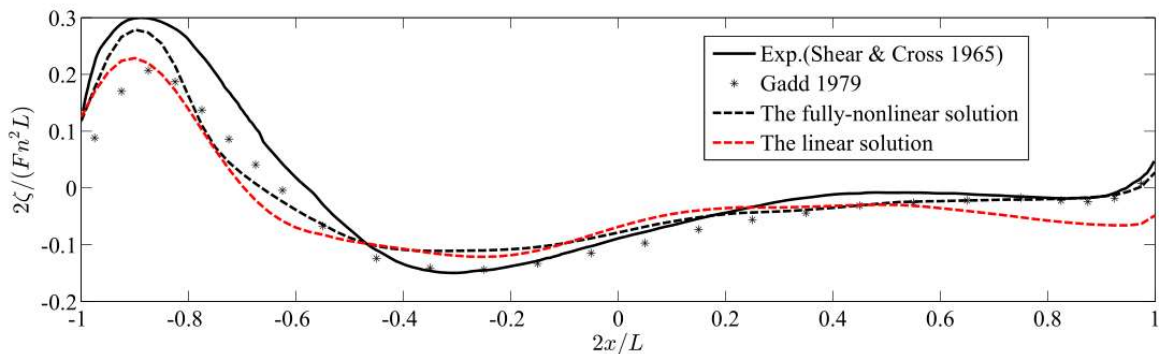


Figure 6. The free-surface elevation along the side of the Wigley hull for $Fn=0.348$. The linear solution uses the Neumann-Kelvin approximation for the free surface conditions.

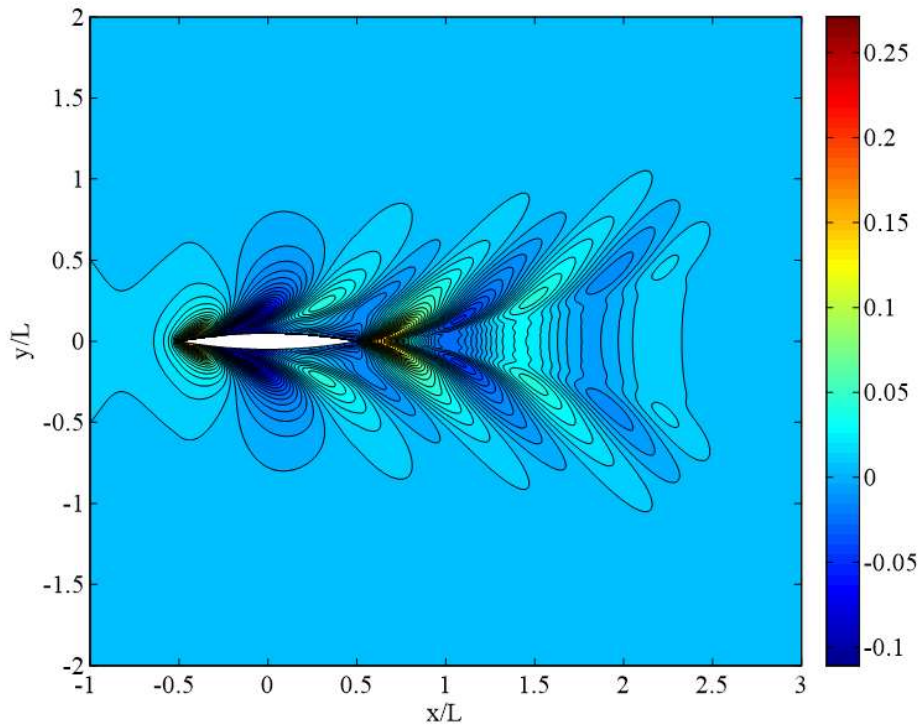


Figure 7. The wave pattern of the Wigley hull travelling at $Fn=0.348$.

the number of the elements on the free surface to about 450,000 and the unknown field points to 4,000,000, which make the fully-nonlinear numerical solver run in a slow speed in the present computer (finishing a time step will cost a few minutes). We may consider developing numerical schemes based on unstructured grids like what we did in the previous cases. It is noted that, for the radiation and diffraction problems, it is not necessary to use the upwind schemes for the advection of the free-surface. This allows to use the unstructured elements on the free-surface boundaries, which may significantly reduce the computational scales.

Summary. A potential-flow solver, based on high-order harmonic polynomials with Cartesian grids with local refinement, is proposed. In the 2D space, many problems including the two cases presented here are solved to verify /validate the solver. It has been demonstrated that the proposed solver is accurate, stable and efficient. In the 3D space, we have done the tests on the linearized radiation and diffraction problems and the linearized problems for the floating bodies moving on the free surface with and without incoming waves. The method behaves stably and efficiently and gives accurate results as long as the grid system well represents the physical flows. We have started solving fully-nonlinear 3D problems to verify and improve the method. As presented in the third case, the method has shown the (potential) capabilities for solving the potential flows of 3D floating bodies moving on the free surface with and without incoming waves stably, accurately and with an acceptable computational speed.

References

- [1] Y.-L. Shao, O. M. Faltinsen, A harmonic polynomial cell (HPC) method for 3D Laplace equation with application in marine hydrodynamics, *J. Comput. Phys.* **274** (2014) 312–332.
- [2] D. G. Dommermuth, D. K. P. Yue, W. M. Lin, R. J. Rapp, E. S. Chan, W. K. Melville, Deep-water plunging breakers: a comparison between potential theory and experiments, *J. Fluid Mech.* **189** (1988) 423–442.
- [3] J. Wang, O.M. Faltinsen, Numerical investigation for air cavity formation during the high-speed water entry of wedges, *J. Offshore Mech. Arct.* **135** (2013) n1.
- [4] J. Wang, C. Lugni, O.M. Faltinsen, Experimental and numerical investigation of a freefall wedge vertically entering the water surface, *Appl. Ocean Res.* **51** (2015) 181–203.
- [5] J. Wang, O.M. Faltinsen, Improved numerical solution of Dobrovolskaya’s boundary integral equations on similarity flow for uniform symmetrical entry of wedges, *Appl. Ocean Res.* **66** (2017) 23–31.
- [6] J. R. Shearer, J.J. Cross, The experimental determination of the components of ship resistance for a mathematic model, R.I.N.A. Report (1965).